

# Identification of Degeneracy, Criticality and Computational Complexity of Two-Dimensional Statistical and Quantum Systems by the Boundary States of Tensor Networks

Shi-Ju Ran,<sup>1</sup> Cheng Peng,<sup>1</sup> Wei Li,<sup>2</sup> and Gang Su<sup>1,\*</sup>

<sup>1</sup>*Theoretical Condensed Matter Physics and Computational Materials Physics Laboratory, School of Physics, University of Chinese Academy of Sciences, P. O. Box 4588, Beijing 100049, China*

<sup>2</sup>*Department of Physics, Beihang University, Beijing 100191, China*

We propose a tensor network (TN)-based theory to address the degeneracy, criticality and computational complexity of two-dimensional (2D) statistical and quantum systems by introducing the boundary thermal state (BTS) and the boundary pure state (BPS) of the TN. The purity of the BTS is robust to identify the degeneracy, say, the system will be non-degenerate if the BTS is pure while it is degenerate if the BTS is mixed. The entanglement of BPS can be utilized to detect the criticality. For gapped systems, the BPS is uncovered to have a finite entanglement entropy  $S$ ; for critical systems,  $S$  is disclosed to increase with the dimension  $D$  of the BPS, exhibiting a logarithmic scaling law  $S = (c/3)\log_2 D + \text{const.}$  with  $c$  the central charge. The scaling law presents an efficient way to determine the central charge of statistical and quantum systems, thereby avoiding the scaling difficulties usually incurred in 2D systems. Our theory also suggests that the computational complexity can be quantified by the entanglement of the BPS. We examine our theory by exact deductions and numerical simulations on several prominent models, where the nearest-neighbour resonating valence bond state on honeycomb lattice is found surprisingly to fall in the same critical universality class as the tricritical Ising model with  $c = 7/10$ . This theory would also have useful implications in studying quantum computations and critical phenomena.

PACS numbers: 71.27.+a, 74.40.Kb, 03.65.Ud

*Introduction.*— The tensor network (TN) provides a powerful framework in different fields. In strongly correlated physics, the TN is considered as a natural representation termed as tensor network state (TNS) [1, 2] for bosonic and fermionic many-body states in two and higher dimensions [3, 4]. The TNS is also known to be capable of describing the states with non-trivial topological properties [5, 6], such as the nearest-neighbor resonating valence bond states [5, 7], string-net condensed states [3], etc. Besides, the TN has also been utilized in quantum computations [9, 10], statistical physics [11], gauge field theories [12], and solving some mathematical problems like counting problems [13], and so on.

Still, the criticality is hard to access since classical simulations on such kind of systems are inefficient even in one dimension (1D) [14]. In addition, to simulate physical properties, e.g. the topological entanglement entropy [15] and the central charge [9, 17], the scaling against the subregion size is needed, which however requires extremely high costs for 2D systems.

Recently, the boundary theories based on the TN representation are quite promising to solve problems that are not easily handled with conventional methods [18, 19]. In quantum many-body physics, the TNS is also expressed as the projected entangled pair state, where the local tensors act as the projectors that map the physical degrees of freedom to virtual ones carrying the entanglement [2]. The inner product of a TNS and its copy  $\langle \psi_{TNS} | \psi_{TNS} \rangle$  is actually the TN after tracing over all physical indexes, and presents a map from a quantum many-body state to its classical correspondence in the same dimension. The resulting classical model can be further mapped onto an effective 1D model. Some theories based on this scheme have been proposed to tackle difficult problems (e.g. identifying the topological orders [18] and simulating

low-energy excitations [19] of 2D quantum systems, etc.).

In this work, we propose a TN-based scheme to address the degeneracy, criticality and computational complexity of 2D statistical and quantum systems by means of the boundary states of the TNs. Using the linearized tensor renormalization group (LTRG) method [20], we express the BTS of the TN in the form of a matrix product operator (MPO) [21], and find that the BTS is pure when the system is non-degenerate, and is mixed if the system is degenerate. Meanwhile, the BPS of the TN can be reached using the matrix product state (MPS) [8] by the infinite time-evolving block decimation (iTEBD) [6, 7] method. We discover that the entanglement entropy ( $S$ ) of the BPS can be utilized to detect the criticality of the system. For gapped systems, the BPS is found to bear only a finite  $S$ , while for critical systems,  $S$  increases with the dimension  $D$  of the BPS, satisfying a logarithmic law

$$S = \frac{c}{3} \log_2 D + \zeta, \quad (1)$$

with  $c$  the central charge [9] and  $\zeta$  a constant. This gives an efficient way to determine the central charge of 2D statistical and quantum systems, while the difficulties in the conventional scaling against the subregion length are avoided. Moreover, our theory suggests that the computational complexity can be quantified by the entanglement entropy of the BPS, showing that the TN's representing gapped states can be efficiently contracted with classical computations.

To examine the validity of our proposal, we perform exact deductions and numerical simulations on several celebrated examples including the 2D Ising model at and away from the critical temperature, the Greenberger-Horne-Zeilinger (GHZ) state [1], the  $Z_2$  topological state [3], the nearest-neighbor resonating valence bond (NNRVB) state [7] on kagomé and

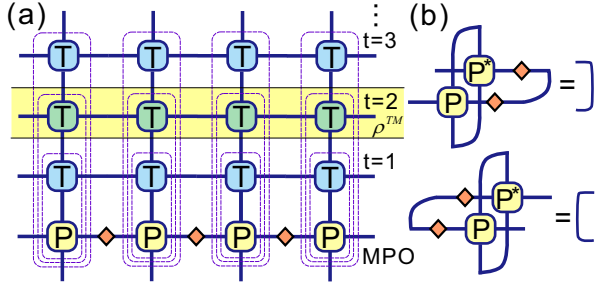


FIG. 1: (Color online) (a) The LTRG scheme on a square TN formed by the local tensor  $T$  and its copies. The contraction of the TN is performed linearly with the help of an MPO formed by local tensors  $P$  and spectrum  $\lambda^O$ . At the  $t$ th renormalization step, each local tensor effectively represents a tensor strip (the dashed circles) containing  $(t + 1)$  original tensors. The transfer matrix  $\rho^{TM}$  of the TN is defined as the tensor stripe along the horizontal direction. (b) The left and right canonical conditions for the MPO.

honeycomb lattices. Surprisingly, we found that the NNRVB state on honeycomb lattice falls in the same critical universality class as the tricritical Ising model with the central charge  $c = 7/10$  [9].

*Tensor network contractions with the boundary states.*— A planar TN is defined in the contraction form as

$$Z = tTr \left( \prod_j T_{u_j l_j d_j r_j}^{[j]} \right), \quad (2)$$

where  $T_{u_j l_j d_j r_j}^{[j]}$  is the local tensors,  $tTr$  is the trace of all common bonds and  $j$  runs over all tensors. Eq. (2) plays a central role in the TN scheme since the calculations of many physical quantities (e.g. the partition function of the 2D classical models [11] or the inner product of two quantum states [2]) is equivalent to computing such a TN contraction. We take the square TN as an example [in Fig. 1 (a)]. Loosely speaking, after contracting the common bonds of some connected tensors in a chosen area [dash squares in Fig. 1 (a)], the size of the resulting tensor increases exponentially with the number of bonds on boundary. It is not clear whether the needed computational cost for an accurate simulation really increase unlimitedly as the area (or the number of boundary bonds) becomes unavoidably larger and larger during the contraction.

The contraction can be implemented linearly. Without losing the generality, we presume the TN satisfies the translational invariance, i.e.  $T_{u_j l_j d_j r_j}^{[j]} = T_{uldr}$ . Let us start with the original local tensor  $P_{uldr}^{(0)} = T_{uldr}$ . For the  $t$ th step of the contraction, the effective tensor  $P^{(t)}$  is updated by contracting one original tensor  $T_{uldr}$  to  $P^{(t-1)}$  as  $P_{ul''d'r''}^{(t)} = \sum_{du'} T_{uldr} P_{u'l'd'r'}^{(t-1)} \delta_{du'}$  with  $l'' = (l, l')$  and  $r'' = (r, r')$ , as shown in Fig. 1 (a). Such a contraction procedure is equivalent to that the LTRG scheme is applied to contract a 2D planar TN instead of performing the imaginary time evolution of the 1D quantum systems [20]. The TN is contracted to an MPO formed by  $P^{(t)}$  and the entanglement spectrum  $\lambda^O$  residing on the virtual bonds. The dimensions of  $l''$  and  $r''$  of  $P$  are bounded in the same way

as that the LTRG bounds the dimensions of the MPO, i.e. the truncations are implemented according to the entanglement spectrum  $\lambda^O$  after canonicalizing the MPO. Similar to the canonicalization of the MPS, the MPO is canonical when the spectrum on any bond is the singular value spectrum between the left/right subregions. The canonical conditions [7] of an MPO in a local form are shown in Fig. 1 (b).

At the  $t$ th step,  $P^{(t)}$  represents efficiently a tensor stripe containing  $t + 1$  original tensors [dash squares in Fig. 1 (a)], and the MPO represents the TN with  $t + 1$  layers. As  $t \rightarrow \infty$ , the MPO converges to the fixed point, i.e.  $P_{ul''d'r''} = \sum_{du'} T_{uldr} P_{u'l'd'r'} \delta_{du'}$ . The fixed point MPO dubbed as the boundary thermal state represents effectively the whole TN.

It is well known that such a contraction of a planar TN can also be done accurately using the MPS with the iTEBD algorithm [2, 7]. After making a sufficiently large number of contractions, one obtains the converged MPS with its local tensor and entanglement spectrum denoted by  $A$  and  $\lambda^S$ . We dub such an MPS that is pure as the boundary pure state (BPS) of the TN. In the following, we show how the BTS and BPS of the TN can be used to identify the degeneracy (of a gapped system) and the criticality of the physical states.

*Purity of the boundary thermal state.*— To proceed, we introduce the transfer operator  $\rho^{TM}$  of the TN defined by the infinite tensor stripe along the direction perpendicular to the contraction direction [the yellow shadow in Fig. 1 (a)] [18, 19]. An essential difference between the MPS-iTEBD and the MPO-LTRG schemes lies in the degeneracy of the dominant eigenvector(s) of  $\rho^{TM}$ . When  $\rho^{TM}$  is non-degenerate, the BPS  $|\psi_{BPS}\rangle$  obtained by the iTEBD algorithm is the dominant eigenvector of  $\rho^{TM}$ , and the MPO  $\hat{\rho}_{BTS}$  in LTRG scheme gives a pure state that is the outer product of  $|\psi_{BPS}\rangle$  and its copy  $\hat{\rho}_{BTS} = |\psi_{BPS}\rangle\langle\psi_{BPS}|$ . In this case, the entanglement spectra  $\lambda^O$  and  $\lambda^S$  of the BTS and BPS have a simple relation  $\lambda^O = \lambda^S \otimes \lambda^S$ . Meanwhile, the contraction of the infinite TN can be reduced to the contraction of the inner product of  $|\psi_{BPS}\rangle$ , which is  $Z = \langle\psi_{BPS}|\psi_{BPS}\rangle$ . This is only the product of the matrices that can be efficiently achieved by classical computers. The computational cost is solely determined by the spectrum  $\lambda^S$ . See more in supplemental material.

When  $\rho^{TM}$  is degenerate, the BTS given by the LTRG scheme is no longer pure, i.e. it cannot be decomposed into an outer product form. The BTS can be formally written in a mixed thermal state  $\hat{\rho}_{BTS} = \sum_{i=1}^{\chi} \eta_i |\phi^i\rangle\langle\phi^i|$  with  $|\phi^i\rangle$  the  $i$ th degenerate eigenvector,  $\eta$  the thermal probability distribution and  $\chi$  the degeneracy. Because the degenerate eigenvectors of  $\rho^{TM}$  correspond to the same eigenvalue, the BTS given by LTRG (which is essentially a power method) is expected to be the maximal mixture of the degenerate states, i.e.  $\eta_i = 1/\chi$ . Meanwhile, it is widely accepted that the BPS  $|\psi_{BPS}\rangle$  by iTEBD favors the minimally entangled state among the combinations of these degenerate eigenvectors. In this case, the canonical spectra of the BTS and BPS do not have a simple outer product relation. Thus we have a way to identify the purity of the BTS by monitoring the spectrum difference  $\varepsilon = |\lambda^O - \lambda^S \otimes \lambda^S|$ .

We observe that the degeneracy of the transfer matrix reflects the degeneracy of the physical models that the TN describes. Interestingly, the BTS gives a mixed state either the degeneracy originates somehow from the spontaneously symmetry-broken states (e.g. the ground states of the Ising model) that obey Landau's paradigm, or from the non-trivial topological degeneracy (e.g. the  $Z_2$  topological state). Thus the purity of the BTS is robust to detect the degeneracy of the system under interest.

*Entanglement scaling of the boundary pure state.*— Besides the purity of the BTS, the entanglement of the BPS by iTEBD can be utilized to detect the criticality of the system. In fact, many works have already been done based on the entanglement of the BPS for the properties of the ground states of 1D quantum models. The subregion length-dependence of the entanglement of a critical state of a spin chain is analogous to that of the entropy in conformal field theories [14]. The entanglement also exhibits the correlation properties of the system and the critical exponents [26] as well as the topological properties, such as the symmetry-protected topological orders [27] and edge excitations [28] in 1D models.

Instead of the 1D quantum chains, we concentrate here on the 2D statistical systems and quantum states that can be written in the TN representations as Eq. (2). As the BPS given by iTEBD is the minimally entangled eigenstate among all the combinations of the degenerate states, its entanglement can be chosen to inspect the criticality. For the gapped systems, we speculate that the entanglement entropy defined as  $S(\lambda^S) = -\sum_i (\lambda_i^S)^2 \log_2 (\lambda_i^S)^2$  saturates to a finite value, and thus only a finite  $D$  is needed. Intuitively, for the critical systems, the entanglement entropy of the BPS should increase with  $D$  unlimedly due to the scaling invariance of such 2D systems, even though the entanglement is minimized in the eigen space. Amazingly, for both the statistical and quantum systems, we found a logarithmic scaling law of the entanglement entropy against  $D$  as Eq. (1), where  $c$  is the central charge that characterizes the criticality in conformal field theory (CFT) [9] and  $\zeta$  is simply a constant.

This scaling scheme against  $D$  surpasses the one against the subregion length  $L$  that reads  $S(\lambda^S) = \frac{c}{3} \log_2 L + \zeta'$  [17] in two ways: (a) the scaling against  $L$  requires an accurate BPS that is hindered by the scaling law itself, as it prevents in principle from an accurate simulation of the BPS with a finite bond dimension; (b) the scaling of  $L$  is available in 1D quantum chain [26], while it is extremely difficult in 2D since the bipartition as well as the calculation of the bipartite quantum entanglement is essentially different from that in 1D.

In our proposal, the BPS is actually the ground state of an effective 1D Hamiltonian  $\hat{H}_{eff}$  defined by the transfer operator  $\rho^{TM} \doteq e^{-\hat{H}_{eff}}$  [18, 19]. We conjecture that  $\hat{H}_{eff}$  shares the same criticality with the original 2D Hamiltonian, thus the criticality of the of the 1D  $\hat{H}_{eff}$  can be used to identify that of the 2D quantum states, thereby avoiding the subregion length scaling in 2D that is usually difficult. Besides, the scaling against  $D$  instead of  $L$  does not require an accurate BPS, thus the conflict to the scaling law is evaded.

*Computational complexity and the equivalence between the dimension and length scalings.*— We find the entanglement entropy  $S(\lambda^S)$  of the BPS can be used to quantify the computational cost, because  $S(\lambda^S)$  indicates the needed dimension cut-off of the BPS to reach the preset accuracy, which is roughly  $D \sim 2^{S(\lambda^S)}$ . For a gapped system, the finiteness of the entanglement entropy indicates that the corresponding TN can be efficiently contracted by a limited cost with classical computers. In contrast, when the system is critical, the increasing entanglement entropy implies that the tensor stripe in the TN cannot be efficiently represented by a local tensor with a finite dimension, thus the TN cannot be contracted efficiently.

Using the relations among  $D$ ,  $L$  and  $S$  mentioned above, we are able to establish an equivalence between the two scaling scenarios against  $L$  and  $D$ , which justify the validity of our scaling scheme for 2D systems. See more details in the supplemental material.

*Two exactly contractible states.*— We illustrate two non-trivial states, the GHZ [1] and  $Z_2$  topological state [3] to examine our proposal. The GHZ state is a topological-trivial state obtained by maximally entangling the two degenerate ground states of the ferromagnetic Ising model. The  $Z_2$  state is the exact ground state of the (gapped) toric-code model which possesses the nontrivial topological order [29]. The inner product TN's of these two states can be exactly contracted.

The local tensor of the inner product TN's of the *priori* unrelated GHZ and  $Z_2$  states can be written in a unified form  $T_{uldr} = \sum_{\mu_1, \mu_2, \mu_3, \mu_4=0}^1 \Lambda_\mu I_{\mu_1, \mu_2, \mu_3, \mu_4} U_{u\mu_1} U_{l\mu_2} U_{d\mu_3} U_{r\mu_4}$ , with  $\Lambda$  the spectrum. We have  $\Lambda_0 = \Lambda_1 = 1/\sqrt{2}$  and  $U$  a  $(2 \times 2)$  unitary matrix (see supplemental material).  $I$  is the so-called super-orthogonal tensor satisfying  $I_{\mu\mu_1\dots} = 1$  if  $\mu = \mu_1 = \dots$  or  $I_{\mu\mu_1\dots} = 0$  otherwise. The matrix  $U$  is actually the rotation matrix satisfying  $U_{0,0} = -U_{1,1} = \cos \theta$  and  $U_{0,1} = U_{1,0} = \sin \theta$  with  $\theta$  the parameter. By taking  $\theta = 0$  and  $0.25\pi$ ,  $U$  becomes the identical and Fourier matrix, which gives the local tensors for the GHZ and  $Z_2$  states, respectively. We note that any translational invariant TN can be exactly contracted when the local tensor bears the same form as the local tensor of the GHZ/ $Z_2$  TN shown above, which actually gives the orthogonal tensor decomposition [5]; the contraction properties of the  $Z_2$  state has been studied from a different perspective using the Hopf algebra [4].

The BTS of the GHZ and  $Z_2$  TNs can also be expressed in a unified form with the local tensor  $P_{uldr} = \sum_{\mu_1, \mu_2} I_{\mu_1, \mu_2, r} U_{u\mu_1} U_{d\mu_2}$  and the spectrum  $\lambda^O = \Lambda$  (see the supplemental material). It is easy to check that the BTS is in the canonical form. Obviously, such a BTS is impure and possesses a finite bond dimension  $D = 2$ , and the canonical entanglement  $\lambda_1^O = \lambda_2^O = 1/\sqrt{2}$ . For the BPS, the MPS converges to an unstable fixed point  $A_{ulr} = \sum_{\mu} I_{\mu, r} U_{u\mu}$  and  $\lambda^S = \Lambda$  only by choosing  $A^{(0)} = I$  as the initial MPS. We have the entanglement entropy of the BPS  $S(\lambda^S) = \log_2 2 = 1$  for both the GHZ and  $Z_2$  states. Otherwise the fixed point flows to the stable fixed point with zero entanglement of the MPS.

We remind that the fixed-point tensor represents effectively

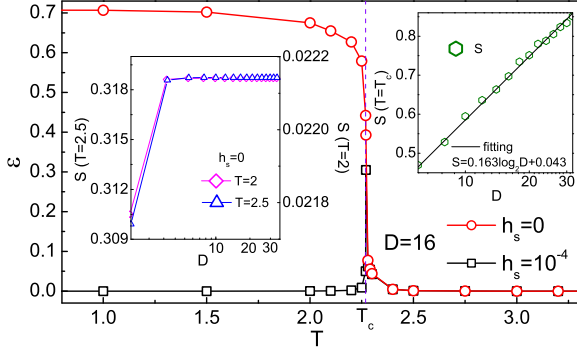


FIG. 2: (Color online) The temperature-dependence of  $\varepsilon = |\lambda^0 - \lambda^S \otimes \lambda^S|$  of the 2D Ising model with and without a small staggered magnetic field  $h_s$ . The two insets show the entanglement entropy  $S$  of the BPS versus its bond dimension  $D$  at  $T = 2, 2.5$  and  $T_c$ . We found that, at  $T = T_c$ , the entanglement entropy  $S$  satisfies  $S(\lambda^S) = 0.163 \log_2 D + 0.043$ , which gives the central charge  $c = 1/2$  according to Eq. (1).

a tensor stripe in the original TN, whose bond dimension is expected to increase exponentially with the stripe length. Instead, we find that the fixed-point tensor (the BTS) has a finite bond dimension  $D = 2$ . This is not surprising for the GHZ state that is just the superposition of two classical ferromagnetic states. In contrast, the quantum entanglement entropy (of the physical degrees of freedom) of the  $Z_2$  state obeys the area law and increases unboundedly as  $S = \alpha L - \gamma$  with  $L$  the boundary length of the subsystem and  $\gamma$  the topological entanglement entropy [15]. Consequently, a large bond dimension  $D$  is expected to capture the quantum entanglement, which scales approximately as  $D \sim 2^S \sim 2^{\alpha L}$ . Despite that, it is quite amazing that the corresponding BPS and BTS only bear a small bond dimension  $D = 2$  with a limited entanglement.

Now we show the absence of the physical degeneracy leads to a pure fixed-point MPO. If we destroy the degeneracy of the two overlapping ferromagnetic states in the GHZ state, we have, equivalently, a shift of  $\Lambda$  as  $\Lambda_2 = \kappa \Lambda_1$  ( $0 < \kappa < 1$ ). Then for the  $t$ th step of renormalization, the canonical spectrum of the MPO satisfies  $\lambda_2^O = \kappa^{(t+1)} \lambda_1^O$ . As  $t \rightarrow \infty$ ,  $\lambda_2^O$  vanishes and the fixed-point MPO becomes a pure state. This picture goes the same as the  $Z_2$  state.

*The 2D Ising model.*— The partition function of the 2D antiferromagnetic (AF) Ising model on square lattice can be written as the contraction of a TN as Eq. (2). The local tensor reads  $T_{uldr} = \exp\{-[s_u s_l + s_l s_d + s_d s_r + s_r s_u + h_s (s_u - s_l + s_d - s_r)]/T\}$ , where  $s_u, s_l, s_d$  and  $s_r$  are the four spins in a plaquette,  $h_s$  is the staggered magnetic field and  $T$  is the temperature.

We study the purity of the BTS at different temperatures by calculating  $\varepsilon = |\lambda^0 - \lambda^S \otimes \lambda^S|$  shown in Fig. 2. For  $T < T_c$  with  $T_c$  the critical temperature, we calculated  $\varepsilon$  in the presence of a small staggered field  $h_s = 10^{-4}$  in order to trigger the  $Z_2$  symmetry breaking, and that at  $h_s = 0$  where the LTRG conserves the  $Z_2$  symmetry. In the first case, we have  $\lambda_0^O = 1$ ,  $\lambda_{s \geq 1}^O = 0$  and  $\lambda^S = \lambda^O$ , which means the BTS is pure with  $\varepsilon = 0$ . In the second case at  $h_s = 0$ , the system contains

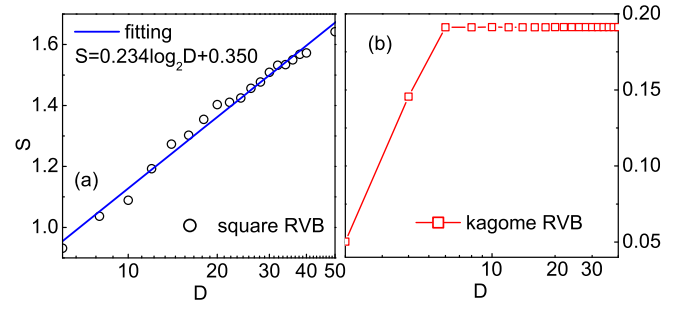


FIG. 3: (Color online) The scaling of the entanglement entropy  $S$  of the BPS against the bond dimension  $D$  for the NNRVB states on (a) honeycomb and (b) kagomé lattices. For the NNRVB state on honeycomb lattice that is critical,  $S$  increases with  $D$  in a logarithmic way as  $S = 0.234 \log_2 D + 0.350$ , giving the central charge  $c = 7/10$  from Eq. (1). The  $S$  of the NNRVB state on kagomé lattice, which is gapped, saturates to  $S \approx 0.19$  as  $D$  increases.

two degenerate states and the BTS flows to a GHZ-like mixed state for  $T < T_c$ . This is evidenced by the obtained spectrum  $\lambda_0^O = \lambda_1^O \approx 1/\sqrt{2}$ ,  $\lambda_{s \geq 2}^O \approx 0$  and  $\lambda_0^S \approx 1$ ,  $\lambda_{s \geq 1}^S \approx 0$ .

For  $T > T_c$ , the MPO flows to a trivial disordered state with or without a staggered field, and the BTS gives a pure state with vanishing  $\varepsilon$ . Consequently, the separating point of the two curves of  $\varepsilon$  gives the critical temperature accurately, where we have  $T_c = 2.27$ , in comparison to the exact critical temperature  $T_c = 2/\ln(1 + \sqrt{2}) \approx 2.269$ . One can also see that at both sides of the critical temperature, the entropy  $S(\lambda^S)$  saturates to a finite value when the bond dimension  $D$  increases, as shown in the left inset of Fig. 2.

At critical temperature  $T_c$ ,  $\varepsilon$  is non-zero (Fig. 2), which indicates that the BTS is a mixed state. We shall remark that the purity of the BTS at the critical point is not robust because an MPO with finite bond dimensions cannot accurately give true BTS of the TN. The right inset in Fig. 2 presents the scaling behavior of  $S(\lambda^S)$  versus  $D$ . It can be seen that the entanglement entropy increases with  $D$  in a logarithmic form as Eq. (1) with  $c \approx 1/2$  and  $\zeta \approx 0.04$ . This is consistent with the former results with CFT [9].

*The topological RVB states.*— The TNS representations of the NNRVB states are given in Ref. [5]. It is known that the NNRVB, which is topological, is critical on bipartite lattices [32] but gapped on non-bipartite lattices [7].

Fig. 3 (a) shows that  $S(\lambda^S)$  of the honeycomb RVB state increases with  $D$  in a logarithmic way as Eq. (1) with the central charge  $c = 7/10$ , which is surprisingly the same as the central charge of the tricritical model [9].

For the kagomé RVB state which is gapped, we find  $\varepsilon \approx 0.1$ , indicating that the BTS is mixed. We also observe  $S(\lambda^S)$  saturates at about  $S(\lambda^S) \approx 0.19$ , evidencing that our theory can identify whether a 2D quantum state is gapped or gapless by the entanglement entropy. We do not see the degeneracy in the entanglement spectrum of the BPS, which we have however seen in the  $Z_2$  state. The reason may be that the corresponding symmetry is not well protected during the contrac-

tion procedure [33].

*Conclusion.*— It is shown that the degeneracy, criticality and computational complexity of the 2D statistical and quantum systems can be effectively addressed in terms of the boundary thermal and pure states of the tensor network. The purity of the BTS and the entanglement entropy of the BPS are used to measure the degeneracy and criticality for both topological and non-topological systems. Importantly, a scaling law against the bond dimension is suggested, with which one can efficiently determine the central charge of 2D statistical and quantum systems. This provides an alternative way to determine the central charge. The computational complexity is discussed, with which an equivalence between the entanglement entropy scalings with bond dimension and subregion length is proposed. The exact deductions and numerical calculations on different kinds of examples give strong supports to our proposal, where we also uncover the NNRVB state on honeycomb lattice falls in the same critical universality class as the tricritical Ising model with the central charge  $c = 7/10$ .

Our proposal may be readily extended to other critical phenomena and gapless quantum systems such as the entropy-driven phase transitions [34], the chiral spin liquids [6] and quantum computations through linearized TN contractions.

This work is supported in part by the MOST of China (Grant No. 2012CB932900 and No. 2013CB933401), the Strategic Priority Research Program of the Chinese Academy of Sciences (Grant No. XDB07010100), and the NSFC (Grant No. 11474279).

---

\* Corresponding author. Email: gsu@ucas.ac.cn

- [1] H. Niggemann, A. Klümper and J. Zittartz, *Z. Phys. B* **104**, 103 (1997); *Eur. Phys. J. B* **13**, 15 (2000).
- [2] F. Verstraete and J. I. Cirac, arXiv:cond-mat/0407066; J. Jordan, R. Orús, G. Vidal, F. Verstraete, and J. I. Cirac, *Phys. Rev. Lett.* **101**, 250602 (2008).
- [3] J. I. Cirac and F. Verstraete, *J. Phys. A: Math. Theor.* **42**, 504004 (2009).
- [4] P. Corboz, J. Jordan and G. Vidal, *Phys. Rev. B* **82**, 245119 (2010).
- [5] F. Verstraete, M. M. Wolf, D. Perez-Garcia, and J. I. Cirac, *Phys. Rev. Lett.* **96**, 220601 (2006).
- [6] T. B. Wahl, H.-H. Tu, N. Schuch, and J. I. Cirac, *Phys. Rev. Lett.* **111**, 236805 (2013).
- [7] D. Poilblanc, N. Schuch, D. Pérez-García, and J. I. Cirac, *Phys. Rev. B* **86**, 014404 (2012); N. Schuch, D. Poilblanc, J. I. Cirac, and D. Pérez-García, *ibid.*, 115108 (2012).
- [8] Z. C. Gu, M. Levin, B. Swingle, and X. G. Wen, *Phys. Rev. B* **79**, 085118 (2009); O. Buerschaper, M. Aguado, and G. Vidal, *ibid.* 085119 (2009).
- [9] I. L. Markov and Y. Y. Shi, *SIAM Journal on Computing* **38**, 963-981 (2008).
- [10] Mear M. R. Koochakie, *Phys. Rev. B* **89**, 012322 (2014).
- [11] M. Levin and C. P. Nave, *Phys. Rev. Lett.* **99**, 120601 (2007).
- [12] L. Tagliacozzo, A. Celi, and M. Lewenstein, *Phys. Rev. Lett.* **4**, 041024 (2014).
- [13] J. D. Biamonte, J. Morton, J. W. Turner, arXiv:cond-mat/1405.7375.
- [14] L. Tagliacozzo, T. R. de Oliveira, S. Iblisdir, and J. I. Latorre, *Phys. Rev. B* **78**, 024410 (2008); F. Pollmann, S. Mukerjee, A. M. Turner, and J. E. Moore, *Phys. Rev. Lett.* **102**, 255701 (2009).
- [15] A. Kitaev and J. Preskill, *Phys. Rev. Lett.* **96**, 110404 (2006); M. Levin and X. G. Wen, *ibid.*, 110405 (2006).
- [16] P. Di Francesco, P. Mathieu, and D. Sénéchal, *Conformal Field Theory* (Springer, Heidelberg, 1999).
- [17] C. Holzhey, F. Larsen, and F. Wilczek, *Nucl. Phys. B* **424**, 443 (1994).
- [18] N. Schuch, D. Poilblanc, J. I. Cirac, and D. Pérez-García, *Phys. Rev. Lett.* **111**, 090501 (2013).
- [19] S. Yang, L. Lehman, D. Poilblanc, K. Van Acoleyen, F. Verstraete, J. I. Cirac, and N. Schuch, *Phys. Rev. Lett.* **112**, 036402 (2014).
- [20] W. Li, S. J. Ran, S. S. Gong, Y. Zhao, B. Xi, F. Ye, and G. Su, *Phys. Rev. Lett.* **106**, 127202 (2011); S. J. Ran, W. Li, B. Xi, Z. Zhang, and G. Su, *Phys. Rev. B* **86**, 134429 (2012).
- [21] B. Pirvu, V. Murg, J. I. Cirac and F. Verstraete, *New J. Phys.* **12** 025012 (2010).
- [22] U. Schollwöck, *Anal. of Phys.* **326**, 96 (2011).
- [23] G. Vidal, *Phys. Rev. Lett.* **91**, 147902 (2003); *Phys. Rev. Lett.* **98**, 070201 (2007).
- [24] R. Orús and G. Vidal, *Phys. Rev. B* **78**, 155117 (2008).
- [25] W. Dür, G. Vidal, and J. I. Cirac, *Phys. Rev. A* **62**, 062314 (2000).
- [26] G. Vidal, J. I. Latorre, E. Rico, and A. Kitaev, *Phys. Rev. Lett.* **90**, 227902 (2003).
- [27] F. Pollmann, A. M. Turner, E. Berg and M. Oshikawa, *Phys. Rev. B* **81**, 064439 (2010).
- [28] X. L. Qi, H. Katsura, and Andreas W. W. Ludwig, *Phys. Rev. Lett.* **108**, 196402 (2012).
- [29] A. Y. Kitaev, *Ann. Phys.* **303**, 2-30 (2003).
- [30] J. Chen and Y. Saad, *SIAM. J. Matrix Anal. & Appl.* **30**, 1709-1734 (2009).
- [31] S. J. Denny, J. D. Biamonte, D. Jaksch and S. R. Clark, *J. Phys. A: Math. Theor.* **45** 015309 (2012).
- [32] A. F. Albuquerque and F. Alet, *Phys. Rev. B* **82**, 180408 (2010); H. Ju, A. B. Kallin, P. Fendley, M. B. Hastings, and R. G. Melko, *ibid* **85**, 165121 (2012).
- [33] A. Weichselbaum, *Anna. of Phys.* **327**, 2972C3047 (2012); C.-Y. Huang, X. C., and F.-L. Lin, *Phys. Rev. B* **88**, 205124 (2013).
- [34] Q. N. Chen, M. P. Qin, J. Chen, Z. C. Wei, H. H. Zhao, B. Normand, and T. Xiang, *Phys. Rev. Lett.* **107**, 165701 (2011).

## Supplemental Material

### I. Tensor networks of the GHZ and $Z_2$ states

The GHZ [1] state is a highly entangled state which is defined as  $|\psi_{GHZ}\rangle = \frac{1}{\sqrt{2}}(\prod_{i=1}^N |0\rangle_i + \prod_{j=1}^N |1\rangle_j)$  and has been introduced as a source state for quantum computations [2]. The GHZ state in form of a square TNS is

$$|\psi_{GHZ}\rangle = \sum_{\{a,s\}} \prod_n I_{a_n,1a_n,2a_n,3a_n,4} \prod_j I_{s_j a_j a'_j} |s_j\rangle, \quad (3)$$

where  $|s_j\rangle$  with  $s_j = 0, 1$  denotes the up or down eigenstate of the  $j$ th spin and  $\{a\}$  are the ancillary indices.  $I$  is the super-diagonal tensors defined as

$$I_{a_1 a_2 \dots a_n} = \begin{cases} 1, & a_1 = a_2 = \dots = a_n. \\ 0, & \text{otherwise.} \end{cases} \quad (4)$$

The  $Z_2$  topological state is the ground state of  $Z_2$  Hamiltonian  $\hat{H}_{Z_2} = -U \sum_l \prod_{i \in \text{legs of } l} \hat{\sigma}_i^x - t \sum_p \prod_{j \in \text{edges of } p} \hat{\sigma}_j^z$  ( $t \gg U$ ) with  $\hat{\sigma}^\alpha$  the Pauli operator [3]. It is a topologically ordered state with long range entanglement. Its TNS representation is

$$|\psi_{Z_2}\rangle = \sum_{\{a,s\}} \prod_n Q_{a_n,1a_n,2a_n,3a_n,4} \prod_j I_{s_j a_j a'_j} |s_j\rangle, \quad (5)$$

where  $Q$  is

$$Q_{a_n,1a_n,2a_n,3a_n,4} = \begin{cases} 1, & \sum_{\alpha=1}^4 a_{n,\alpha} = \text{even.} \\ 0, & \text{otherwise.} \end{cases} \quad (6)$$

One can see that the TNS of such two states can be written in a unified form

$$|\psi\rangle = \sum_{\{a,s\}} \prod_n F_{a_n,1a_n,2a_n,3a_n,4}^{(n)} \prod_j I_{s_j a_j a'_j}^{(j)} |s_j\rangle, \quad (7)$$

where  $F^{(n)}$  is a tensor defined on the  $n$ th vertex of the network and  $I^{(j)}$  is a super-diagonal tensor [Eq. (4)] on the  $j$ th edge. See FIG. S1 (a). The tensor  $I^{(j)}$  is actually a projector which projects the ancillary indices represented by  $a_j$  and  $a'_j$  to the physical index  $s_j$ .

With the given TNS, a calculation of concerned quantity, such as  $Z = \langle \psi | \psi \rangle$  or  $\langle \hat{O} \rangle = \langle \psi | \hat{O} | \psi \rangle / Z$  with  $\hat{O}$  a quantum operator, becomes the contraction of a corresponding TN. For the TN of  $Z$ , the

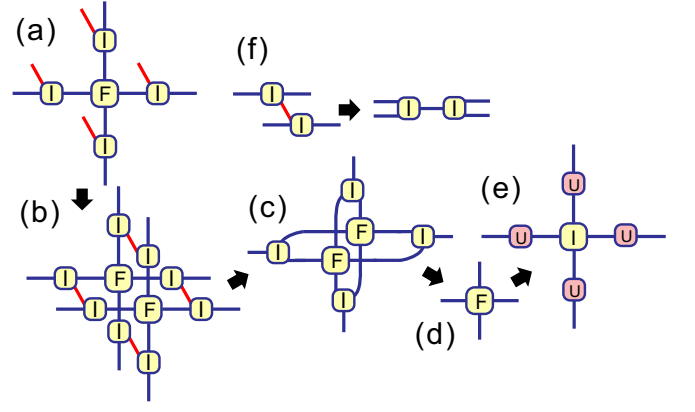


FIG. S1: (Color online) (a) The unified TNS representation of the GHZ and  $Z_2$  state [Eq. (7)]. (b) The sketch of the inner product TN  $Z = \langle \psi | \psi \rangle$ . (c) The TN  $Z$  can be transformed with Eq. (8) into a TN formed by the local tensor  $F$  shown in (d). (e)  $F$  can be decomposed by the orthogonal tensor decomposition with Eq. (10). (f) The eigenvalue decomposition of the tensor  $I$  [Eq. (9)].

local tensor satisfies [FIG. S1 (c)]

$$T_{g_n,1g_n,2g_n,3g_n,4}^{(n)} = \sum_{a,b} F_{a_n,1a_n,2a_n,3a_n,4}^{(n)} F_{b_n,1b_n,2b_n,3b_n,4}^{(n)*} I_{a_n,1b_n,1g_n,1}^{(n,1)} I_{a_n,2b_n,2g_n,2}^{(n,2)} I_{a_n,3b_n,3g_n,3}^{(n,3)} I_{a_n,4b_n,4g_n,4}^{(n,4)}, \quad (8)$$

where  $I_{a_n,jb_n,jg_n,j}^{(n,j)}$  ( $j = 1, 2, 3, 4$ ) is obtained by the eigenvalue decomposition [FIG. S1 (f)]

$$\sum_{s_n,j} I_{s_n,j a_n,j a'_n,j}^{(n,j)} I_{s_n,j b_n,j b'_n,j}^{(n,j)} = \sum_{g_n,j} I_{a_n,j b_n,j g_n,j}^{(n,j)} I_{a'_n,j b'_n,j g_n,j}^{(n,j)}. \quad (9)$$

When taking the local tensor  $P^{(n)}$  as the one in Eq. (3) or Eq. (5), one readily has  $T^{(n)} = F^{(n)}$  in Eq. (8) according to the tensor fusion algebra [4]. Meanwhile, we found that  $T^{(n)}$  can be decomposed by orthogonal tensor decomposition [5] as

$$T_{a_n,1a_n,2a_n,3a_n,4}^{(n)} = \sum_{r=0}^1 \Lambda_r^{(n)} U_{a_n,1r} U_{a_n,2r} U_{a_n,3r} U_{a_n,4r}, \quad (10)$$

The matrix  $U$  for GHZ and  $Z_2$  TN is actually the rotation matrix

$$U = \begin{bmatrix} \cos(\theta) & \sin(\theta) \\ \sin(\theta) & -\cos(\theta) \end{bmatrix} \quad (11)$$

with  $\theta$  the parameter.  $U$  is orthogonal which satisfies

$$I_{rr'} = \sum_a U_{ar} U_{ar'}. \quad (12)$$

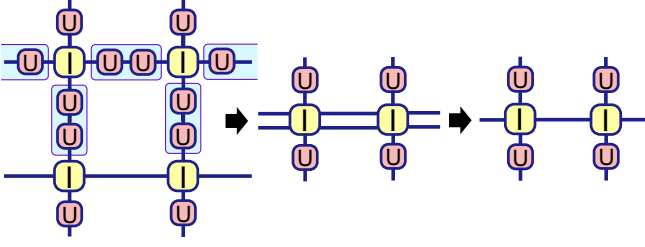


FIG. S2: (Color online) The sketch that shows the fixed point MPO. For the first arrow, we apply the orthogonality  $UU^T = I$ , and for the second arrow, we apply the equations  $\sum_{\mu} I_{\mu\mu_1\dots\mu_{\mu_1\dots}} = I_{\mu_1\dots\mu_2\dots}$  and  $\sum_{\mu\mu'} I_{\mu\mu'\dots} I_{\mu'\mu''\dots} = \sum_{\mu} I_{\mu\dots} I_{\mu''\dots}$ .

By taking  $\Lambda^{(n)} = \Lambda = [1/\sqrt{2}, 1/\sqrt{2}]$  in Eq. (10) and  $\theta = 0$  in Eq. (11), one obtains the GHZ state with Eq. (7) and the corresponding local tensor of  $Z$  with Eq. (10). By taking  $\Lambda = [1/\sqrt{2}, 1/\sqrt{2}]$  and  $\theta = \pi/4$ , one has the  $Z_2$  topologically ordered state and the local tensor of  $Z$ . Comparing these two states, both of them are highly entangled, while the GHZ state was introduced for quantum teleportation and the  $Z_2$  state was revealed to bear a non-trivial topological entanglement. But against expectations, such two states belong to the same class characterized by only one parameter  $\theta$ .

## II. The fixed-point MPO of the GHZ/ $Z_2$ tensor networks

FIG. S2 illustrates the proof of the fixed point of the GHZ and  $Z_2$  TN with LTRG. The local tensor of the MPO satisfies

$$P_{a_1 a_2 a_3 a_4} = \sum_{r=0}^1 \Lambda_r U_{a_1 r} I_{a_2 r} U_{a_3 r} I_{a_4 r}, \quad (13)$$

and the entanglement spectrum is  $\lambda^O = \Lambda$ . During the contraction, the adjacent matrices  $U$ 's vanish according to Eq. (12), and by applying  $\sum_{\mu} I_{\mu\mu_1\dots\mu_{\mu_1\dots}} = I_{\mu_1\dots\mu_2\dots}$  and  $\sum_{\mu\mu'} I_{\mu\mu'\dots} I_{\mu'\mu''\dots} = \sum_{\mu} I_{\mu\dots} I_{\mu''\dots}$ , the resulting MPO is exactly the same as the one before the contraction. This proof holds for both GHZ and  $Z_2$  TNs by taking  $\theta = 0$  and  $\pi/4$  in  $U$  [Eq. (11)].

## III. Computational complexity and the equivalence of two entanglement entropy scaling scenarios

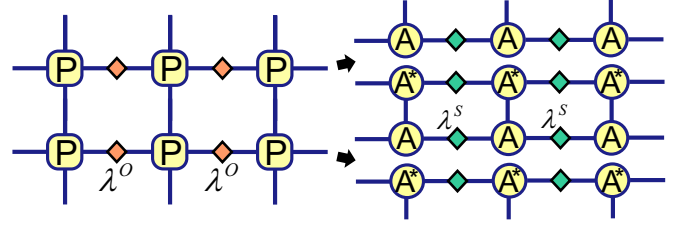


FIG. S3: (Color online) When the BTS is pure, it can be decomposed into the outer product of the BPS and its copy with  $A$  and  $\lambda^S$  the local tensor and the entanglement spectrum, respectively. The TN contraction simply becomes the inner product of the corresponding MPS that can be efficiently simulated.

The transfer matrix  $\rho^{TM}$  of a TN is defined as an infinite tensor stripe across the TN, so that the TN contraction can be rewritten as the product of the  $\rho^{TM}$  as  $Z = \text{Tr}[\lim_{n \rightarrow \infty} (\rho^{TN})^n]$ . Meanwhile, the  $\rho^{TM}$  also defines a 1D effective Hamiltonian as  $\rho^{TM} \doteq e^{-\hat{H}_{eff}}$ . When the ground state of  $\hat{H}_{eff}$  is unique, its “zero-temperature” thermal state, dubbed as the boundary thermal state (BTS) and defined as  $\hat{\rho}_{BTS} \doteq \lim_{\beta \rightarrow \infty} e^{-\beta \hat{H}_{eff}}$ , is pure, where  $\beta$  is the effective inverse temperature. In other words,  $\hat{\rho}_{BTS}$  is the outer product of the ground state  $|\phi_{BPS}\rangle$  (dubbed as the boundary pure state, BPS) of  $\hat{H}_{eff}$ , i.e.  $\hat{\rho}_{BTS} = |\phi_{BPS}\rangle\langle\phi_{BPS}|$ . In this case as shown in FIG. S3, the TN contraction is reduced to the computation of the inner product of  $|\phi_{BPS}\rangle$ . By the infinite time-evolving block decimation (iTEBD) [6, 7] method,  $|\phi_{BPS}\rangle$  can be efficiently obtained, which is written in a matrix product state (MPS) [8]. Then the inner product of  $|\phi_{BPS}\rangle$  is only the product of matrices whose computational complexity totally relies on the entanglement spectrum  $\lambda^S$  of the MPS.

Approximately, the computational cost can be quantified by entanglement entropy of the MPS which is defined as  $S(\lambda^S) = -\sum_i (\lambda_i^S)^2 \log_2 (\lambda_i^S)^2$ . We have that the needed dimension  $D$  for an accurate simulation satisfies

$$D \sim 2^{S(\lambda^S)}. \quad (14)$$

To see this, we apply it to the simplest situation where the spectrum is flat, say  $\lambda_0^S = \dots = \lambda_{D-1}^S = D^{-0.5}$  and  $\lambda_{s \geq D}^S = 0$ . The normalizing condition  $|\lambda^S| = 1$  is fulfilled. Obviously the needed dimension is  $D$ , and the entanglement entropy is  $S(\lambda^S) = -(D/D) \log_2 (D^{-1}) = \log_2 D$  exactly. Then we have  $D = 2^{S(\lambda^S)}$ . One can check this relation also holds approximately when the entanglement spectrum is

not flat by presetting a precision for cutting the dimension.

It has been given for critical 1D quantum states by the conformal field theory, that the scaling of the entanglement entropy versus the subregion length  $L$  satisfies a logarithmic law

$$S = \frac{c}{3} \log_2 L + \text{const.}, \quad (15)$$

with  $c$  the central charge which characterizes the critical universality class [9]. By combining Eqs. (14) and (15), one readily has

$$S = \frac{c}{3} \log_2 D + \text{const.}, \quad (16)$$

which gives the equivalence between the  $S(\lambda^S)$ -scaling against  $L$  and that against  $D$ .

---

\* Corresponding author. Email: gsu@ucas.ac.cn

- [1] W. Dür, G. Vidal, and J. I. Cirac, Phys. Rev. A **62**, 062314 (2000).
- [2] D. Gottesman and I. L. Chuang, nature **402**, 390-393 (1999).
- [3] Z. C. Gu, M. Levin, B. Swingle, and X. G. Wen, Phys. Rev. B **79**, 085118 (2009); O. Buerschaper, M. Aguado, and G. Vidal, *ibid.* 085119 (2009).
- [4] S. J. Denny, J. D. Biamonte, D. Jaksch and S. R. Clark, J. Phys. A: Math. Theor. **45** 015309 (2012).
- [5] J. Chen and Y. Saad, SIAM. J. Matrix Anal. & Appl. **30**, 1709-1734 (2009).
- [6] G. Vidal, Phys. Rev. Lett. **91**, 147902 (2003); Phys. Rev. Lett. **98**, 070201 (2007).
- [7] R. Orús and G. Vidal, Phys. Rev. B **78**, 155117 (2008).
- [8] U. Schollwöck, Anal. of Phys. **326**, 96 (2011).
- [9] P. Di Francesco, P. Mathieu, and D. Sénéchal, *Conformal Field Theory* (Springer, Heidelberg, 1999).